

Two-Photon Absorption from the Real Gaussian Field

Ce Chen and D. S. Elliott

School of Electrical Engineering, Purdue University, West Lafayette, Indiana 47907

M. W. Hamilton^(a)

Department of Physics and Applied Physics, University of Strathclyde, Glasgow, G40NG, Scotland

(Received 4 November 1991)

We have measured the absorption line shape for two-photon absorption from a broadband field known as the real Gaussian field. We observe that, in the case of large optical bandwidth, the width of the absorption spectrum is narrower than that of the optical field. Agreement with calculated line shapes and widths is excellent.

PACS numbers: 42.50.Ar, 32.70.Jz, 32.80.Wr

We report measurements of two-photon absorption from a spectrally broadened laser field known as the real Gaussian field. Much recent work has considered the effects of external noise on a variety of physical processes. For example, quantum systems whose classical counterparts exhibit chaotic behavior have recently been shown [1] to tend towards classical behavior (delocalization and diffusion of expectation values) when driven by a weak external noise force. Other examples are found in dynamical behavior of laser systems [2], atomic transitions induced by squeezed light [3], and blackbody radiation-induced atomic transitions and Stark shifts [4].

In the case of multiphoton absorption it is well known [5-8] that the transition rate is enhanced in going to a thermal field from a coherent field. Both the linewidth and line shape of the field have an effect on the absorption spectra for nonlinear interactions [9,10]. But more importantly, the nonlinear absorption spectrum depends on the detailed characteristics of the fluctuations of the field which lead to its spectral broadening [9,11]. For example, phase and amplitude fluctuations can result in the same laser spectrum, but give qualitatively different two-photon absorption spectra. For the case of the real Gaussian field we observe an unusual dependence of the absorption width on the laser width. In the limit of large laser bandwidth, the width of the absorption spectrum is actually narrower than the spectral width of the laser. This is in marked contrast to the behavior observed in Ref. [10] for the phase diffusing field where the width of the absorption spectrum increases linearly with that of the laser.

This work is made possible by a technique that we have developed [12] for statistically controlling the laser noise in a detailed way. The real Gaussian field is characterized by a fluctuating amplitude $\epsilon(t)$ and a fixed frequency ω_0 :

$$E(t) = \epsilon(t)e^{-i\omega_0 t} + \text{c.c.} \quad (1)$$

In this expression $\epsilon(t)$ is real and Gaussian, and fluctuates about a mean value of zero. We generate this field [12] by driving an acousto-optic modulator (AOM) with a rf (200 MHz) voltage of the form of Eq. (1). A cw,

frequency-stabilized laser beam incident on the acousto-optic crystal at the Bragg angle is diffracted by the acoustic wave, forming the real Gaussian field, whose frequency is shifted from the incident laser frequency by 200 MHz. In order to preserve the statistical properties of the signal, we limit the diffraction efficiency of the AOM to about 2%. Since the power damage threshold of the acousto-optic crystal is 200 mW, the optical power in the real Gaussian field is limited to about 4 mW.

The power spectrum of the real Gaussian field is shaped to that of a Lorentzian function

$$P(\omega) = \frac{2\epsilon_0^2/\beta}{1 + [(\omega - \omega_0)/\beta]^2}, \quad (2)$$

where 2β is the full width at half maximum (FWHM), and ϵ_0 is the root-mean-square amplitude of the field. The bandwidth of the real Gaussian field is controlled by filtering the noise voltage used to generate the real Gaussian drive voltage. For the work reported here, the laser bandwidth (FWHM) is $\beta/\pi = 2.6, 5.2, 11.0,$ and 16.0 MHz. Using a confocal Fabry-Pérot cavity we estimate the bandwidth of the unmodulated output of the laser field to be less than 0.5 MHz.

In order to calculate the two-photon absorption spectrum from this field, we use the results of Mollow [9], who used a second-order perturbative approach to show that the two-photon absorption spectrum is given by

$$W(\omega_0) = 2|g(\omega_0)|^2 \int_{-\infty}^{\infty} dt e^{2i\omega_f t - \kappa|t|} G^{(4)}(-t, -t; t, t). \quad (3)$$

In this expression $g(\omega_0)$ is the two-photon transition moment, $\hbar\omega_f$ and κ are the energy and FWHM of the excited state, and $G^{(4)}$ is the fourth-order field correlation function. Mollow evaluated the absorption spectra for a phase diffusion field and a thermal field. For the real Gaussian field, the fourth-order correlation function can be shown to be of the form

$$G^{(4)}(-t, -t; t, t) = \epsilon_0^4 (1 + 2e^{-4\beta|t|}) e^{-4i\omega_0 t}. \quad (4)$$

The first term in this correlation function represents a nondecaying coherence induced because the field ampli-

tude is real. Using Eqs. (3) and (4), the absorption spectrum is

$$W(\omega_0) = |g(\omega_0)|^2 \epsilon_0^4 \left\{ \frac{\kappa/4}{(\omega_f/2 - \omega_0)^2 + (\kappa/4)^4} + 2 \frac{\kappa/4 + \beta}{(\omega_f/2 - \omega_0)^2 + (\kappa/4 + \beta)^2} \right\}. \tag{5}$$

The absorption line shape is the sum of two Lorentzians. The first term, representing $\frac{1}{3}$ of the total area, has a width limited only by the atomic width $\kappa/2$ (FWHM). This term comes from the constant term in the correlation function in Eq. (4). The second term has $\frac{2}{3}$ of the total peak area, and has a width equal to the sum of the atomic width and laser width 2β . In the case of $\beta \gg \kappa/4$, the second term becomes very broad, and its peak height decreases correspondingly. The dominant feature which remains is the first term, which is of width $\kappa/2$. Thus for this field we see a prediction of an absorption feature whose width can be much less than the width of the field from which the light is being absorbed.

The measurements of the laser bandwidth effects were carried out using the $3s \ ^2S_{1/2}(F=2) \rightarrow 5s \ ^2S_{1/2}(F=2)$ two-photon transition in atomic sodium. See Fig. 1 for a diagram of the relevant energy levels of sodium. The two-photon transition wavelength (602 nm) in sodium is 13 nm from the single-photon $3S \rightarrow 3P$ resonance wavelength, so direct excitation of the $3P$ state is negligible. The $3s \ ^2S_{1/2}(F=1) \rightarrow 5s \ ^2S_{1/2}(F=1)$ is also an allowed transition in our configuration. This transition is at a laser frequency 808 MHz higher than that of the $F=2$ transition, and does not influence our measurements. The rate of two-photon absorption by the atomic sodium was monitored by detecting the fluorescent decay of the $5s$ state. The $5s$ state decays by way of the 4^2P state with a

branching ratio [13] of 0.43, generating a fluorescence signal at 330 nm, corresponding to the second step of the decay ($4P \rightarrow 3S$).

The experimental configuration is shown in Fig. 2. In the first AOM, the real Gaussian field was generated as discussed above. The undiffracted field from this AOM was focused into the second AOM to produce a laser beam which was used to lock the laser frequency to the sodium transition frequency. Each of these beams, which we will refer to as the signal beam and locking beam, respectively, was focused into heated sodium cells ($T = 160^\circ\text{C}$). From each sodium cell, we collected the fluorescent radiation using a $f = 25$ mm quartz lens (clear aperture ~ 15 mm), which focused the fluorescence radiation onto an aperture, behind which was placed an interference filter (peak transmission at 330 nm) and photomultiplier. The collection lens was positioned ~ 50 mm from the interaction region, forming a collection solid angle of ~ 0.07 sr. The aperture was used to reduce the background light, which arose principally from scattering of the laser light at the entrance and exit windows of the cell. The photomultiplier used to detect the 330-nm signal had a 30% quantum efficiency and a current gain of $\sim 10^7$.

We used a technique for locking and scanning the laser similar to a standard technique [14] employing frequency

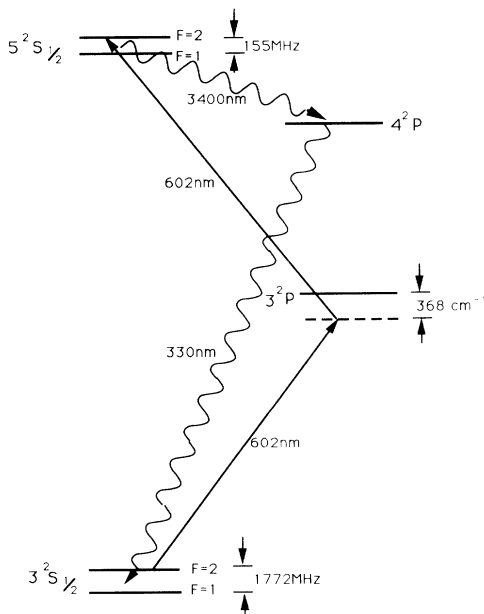


FIG. 1. Energy-level diagram of sodium showing the spectroscopic data relevant to this experiment.

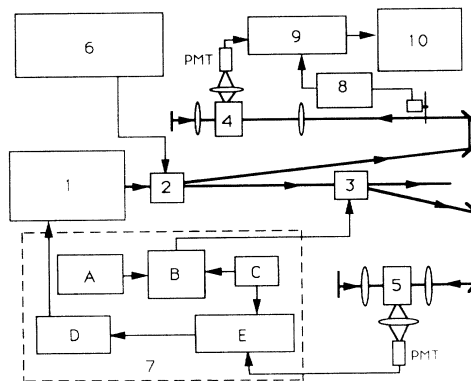


FIG. 2. Experimental configuration for the two-photon absorption measurements. The numbered components are as follows: 1, stabilized tunable ring dye laser; 2 and 3, acousto-optic modulators; 4 and 5, sodium vapor cells; 6, rf electronics for generating the real Gaussian field; 7, control electronics for locking and scanning the laser frequency through the two-photon transition (consisting of a ramp generator *A*, voltage-controlled oscillator *B*, frequency dither source *C*, a voltage integrator *D*, and lock-in amplifier *E*); 8, beam chopper driver; 9, lock-in amplifier; and 10, laboratory computer.

modulation of the locking beam and phase-sensitive detection of the fluorescence light. This technique was applied here to lock to the two-photon transition. An error signal thus generated tuned the laser frequency to maintain resonance between the locking beam and the sodium transition. The signal beam was indirectly tuned through resonance by varying the rf frequency of the locking-beam AOM drive voltage. The frequency of the signal-beam AOM drive voltage was not varied. The detuning of the signal beam from the transition is easily determined and accurately calibrated, since it is simply the difference between the center drive frequencies of the two AOM's. Linearity of the scan is assured by the tuning characteristics of the rf oscillator. The long-term stability of the laser frequency was excellent, allowing long-

duration scans without concern of drift.

The signal beam was chopped at ~ 530 Hz to improve sensitivity, and focused into a sodium cell with a lens of focal length $f=15$ cm. The beam exiting the cell was collimated, reflected, and refocused back into the cell, as is standard for Doppler-free two-photon absorption measurements. The round-trip delay time of the reflected beam from the interaction region to the reflector and back to the interaction region was ~ 1 nsec, much less than the correlation time of the field. The fluorescence signal was amplified with a lock-in amplifier, whose output was digitized and stored on a PC AT laboratory computer. The frequency scan ramp was stored concurrently. The total frequency scan of about 35 MHz took 14 min. The absorption spectra were recorded four times for each

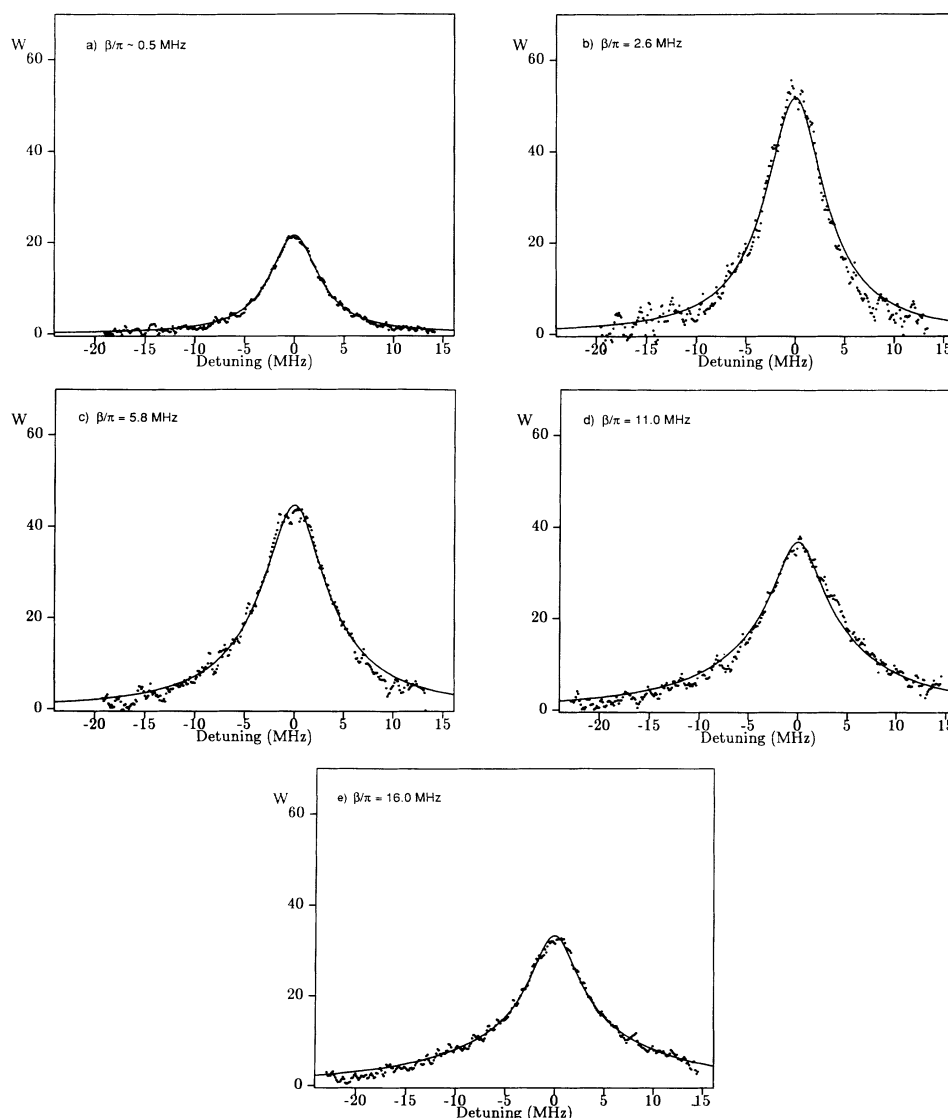


FIG. 3. Two-photon absorption spectra. The laser bandwidth is given for each of the spectra. For (a), the field is the coherent field. The solid line is the line shape given by Eq. (5) in the text.

of the four real Gaussian field bandwidths used, and three times with coherent light. For the coherent light measurements the first AOM was driven directly with the unmodulated output of a 200-MHz signal generator. The averages for each of the data sets are shown as the data points in Fig. 3. These data have been normalized by the square of the laser power, which ranged from 2.6 to 4.0 mW for the "noisy" fields, and was 5.7 mW for the coherent light data. The atomic width $\kappa/4\pi$ for this work was measured to be 6.0 MHz, limited by the 2-MHz natural linewidth of the atom, and by collisional broadening. (The collisional broadening rate of the $5S$ state of sodium with helium, for example, is very large [15], ~ 95 MHz/torr. Estimates of other possible broadening processes, such as transit time broadening, ionization lifetime broadening, or Stark broadening, are much smaller than the observed width.)

The solid lines in Fig. 3 represent the line shape given by Eq. (5). These curves are not fitted to the data, except for a small adjustment to the amplitude, and a 0.3-MHz shift of the center frequency (this is within the uncertainty of measurements). The data and the calculated curves are in excellent agreement. Figure 3(e) shows the unusual behavior of the absorption width referred to earlier. In this figure, the laser width is $\beta/\pi = 16.0$ MHz, and the width of the absorption peak is only 10 MHz.

We have also measured the enhancement in the resonant absorption rate when induced by the real Gaussian field as compared to the absorption rate from a coherent field of the same average intensity. For each of the laser bandwidths of our experiment, we find good agreement between measured and calculated enhancement factors. These results will be discussed in more detail in a future report.

We conclude by briefly mentioning two related cases. For a complex Gaussian field, as is produced by any thermal source, the long-term coherence of the field is not present, and the absorption spectrum reduces to only the second term in Eq. (5). Future work is planned in our laboratory to observe this feature. Finally, we note that these observations of two-photon absorption from the real Gaussian field imply that a similar absorption process from a squeezed optical state should also display an absorption spectrum which contains a term limited only by the atomic linewidth.

This work was supported by the Department of Energy, Office of Basic Energy Sciences, and through a Presidential Young Investigator Award from the National Science Foundation. Participation by M.W.H. was made possible by a Collaborative Research Grant from the NATO Scientific Affairs Division.

^(a)Present address: Department of Physics, University of Adelaide, Adelaide, SA5000, Australia.

- [1] See, for example, R. Blümel, A. Buchleitner, R. Graham, L. Sirko, U. Smilansky, and H. Walther, *Phys. Rev. A* **44**, 4521 (1991); J. E. Bayfield and D. W. Sokol, *Phys. Rev. Lett.* **61**, 2007 (1988).
- [2] G. P. Agarwal, *Phys. Rev. A* **37**, 2488 (1988); G. P. Agarwal and R. Roy, *Phys. Rev. A* **37**, 2495 (1988); G. Gray and R. Roy, *Phys. Rev. A* **40**, 2452 (1989).
- [3] C. W. Gardiner, *Phys. Rev. Lett.* **56**, 1917 (1986); H. Ritsch and P. Zoller, *Phys. Rev. Lett.* **61**, 1097 (1988).
- [4] T. F. Gallagher and W. E. Cooke, *Phys. Rev. Lett.* **42**, 835 (1979); W. P. Spenser, A. G. Vaidyanathan, D. Kleppner, and T. Ducas, *Phys. Rev. A* **25**, 380 (1982).
- [5] F. Shiga and S. Imamura, *Phys. Lett.* **25A**, 706 (1967).
- [6] J. Krasinski, S. Chudzynski, W. Majewski, and M. Glod, *Opt. Commun.* **12**, 304 (1974).
- [7] C. Lecompte, G. Mainfray, C. Manus, and F. Sanchez, *Phys. Rev. Lett.* **32**, 265 (1974); *Phys. Rev. A* **11**, 1009 (1975).
- [8] T. U. Arslanbekov, N. B. Delone, A. V. Masalov, S. S. Todirasku, and A. G. Fainshtein, *Zh. Eksp. Teor. Fiz.* **72**, 907 (1977) [*Sov. Phys. JETP* **45**, 473 (1977)].
- [9] B. R. Mollow, *Phys. Rev.* **175**, 1555 (1968).
- [10] D. S. Elliott, M. W. Hamilton, K. Arnett, and S. J. Smith, *Phys. Rev. Lett.* **53**, 439 (1984); *Phys. Rev. A* **32**, 887 (1985).
- [11] R. Boscaino and R. N. Mantegna, *Opt. Commun.* **73**, 289 (1989).
- [12] Cheng Xie, G. Klimeck, and D. S. Elliott, *Phys. Rev. A* **41**, 6376 (1990).
- [13] A. Lindgård and S. E. Nielsen, *At. Data Nucl. Data Tables* **19**, 533 (1977).
- [14] R. V. Pound, *Rev. Sci. Instrum.* **17**, 490 (1946); R. W. P. Drever, J. L. Hall, F. V. Kowalski, J. Hough, G. M. Ford, A. J. Munley, and H. Ward, *Appl. Phys. B* **31**, 97 (1983).
- [15] A. Flusberg, R. Kachru, T. Mossberg, and S. R. Hartmann, *Phys. Rev. A* **19**, 1607 (1979).